Experimental study of operating regimes in a vapor chamber with integrated hollow fins

Elise Bérut, Stéphane Lips, Frédéric Lefevre, Valérie Sartre

Experimental study of operating regimes in a vapor chamber with integrated hollow fins

Bérut E., Lips S., Lefèvre F., Sartre V.

Univ Lyon, INSA Lyon, CNRS, CETHIL UMR5008, F-69621 Villeurbanne, France

E-mail: elise.berut@insa-lyon.fr

Abstract. A thermosyphon vapor chamber was manufactured and tested. The evaporator is made of copper and has a circular geometry (185 mm outer diameter). The condenser consists of an array of hollow fins made of 300 µm thick polymer layer and having an inner diameter ranging from 5.3 to 10.7 mm. It is cooled by forced convection. Experiments were carried out to characterize operating regimes depending on the working fluid, fins diameter, fluid fill charge and heat flux. HFE-7100, n-pentane and water were tested. Visualizations were made, as well as temperature and pressure measurements over time. For HFE and pentane, a stable oscillating regime was observed for all operating conditions, with film condensation and nucleate boiling. For water, dropwise condensation occurs and many hydrodynamic phenomena were observed depending on the operating conditions (geyser effect, liquid plugs, flooding of tubes), leading to intermittent behaviors. Operating regime maps are proposed. The influence of the regimes on the thermal performance of the vapor chamber is small as long as the fin inner diameter is large enough to prevent the occurrence of stable liquid plugs occupying the whole height of the tubes. The determination of the critical diameter is thus of great importance for the performance optimization, considering condensation heat transfer as well as external convection.

1. Introduction

With the decrease in the size of electronic components leading to ever-increasing heat flux levels, thermal management has become a major concern in the electronic industry. Heat pipes and vapor chambers have proven to be amongst the most efficient passive cooling devices [1] but the research is ongoing to improve the design of these systems.

Traditionally, vapor chambers are used as heat spreaders and associated with solid air-cooled finned heat sinks. The heat sink is then placed directly above the condensation zone. For this study however, a vapor chamber with integrated hollow fins was built and tested. This condenser design has the following benefits: no contact thermal resistance between the vapor chamber and the finned region, and high fin efficiency. Thanks to the fluid condensation inside the fins, they are indeed virtually isothermal, resulting in better thermal performance compared to traditional air-cooled heat sinks.

This type of configuration has been barely studied in the literature. Such systems seem to be first mentioned in 2007, when Michels *et al.* [2] presented an analytical model to predict the thermal resistances of a vapor chamber with hollow fins. Michels *et al.* also obtained experimental data in 2012 [3]. Three other experimental studies were conducted on the same topic from 2010 to 2017 [4-6] using distilled water as the working fluid.

The main objective of this work is to characterize the different operating regimes that may arise in vapor chambers with hollow fins depending on the working fluid, the fin diameter, the fluid fill charge and the

heat flux. Thanks to a transparent condenser, the hydrodynamic phenomena can be visualized for the first time in such systems, to our knowledge. The impact of the regimes on the thermal resistance is also studied.

2. Experimental setup

2.1. Experimental setup description

Figure 1 shows a picture of the prototype, which has a circular geometry. It was designed so that the condenser can be easily changed in order to test several fin diameters. Three condensers were studied, having 14 cm high fins with 5.3, 7.6 and 10.7 mm inner diameter. The thickness of the tubes wall, made of polymer polyethylene terephthalate (PET), is 300 µm. The fins are glued to a transparent polycarbonate cover. The condenser and copper evaporator are clamped together, with a 156 mm inner diameter seal between them to form a vacuum tight vapor space, which is 13 mm high. To prevent deformation of the tubes and of the cover, the saturation temperature must not exceed 55 °C and the operating pressure must be kept slightly under the atmospheric pressure.

The heat source is a resistive heater, 90 mm in diameter, supplying total heat transfer rates up to 150 W (2.4 W/cm²). It is thermally insulated. The condenser is air cooled by fans placed in a steel duct. The air temperature is maintained at 22.5 ± 1.5°C and its velocity is around 3.5 m/s. Visualizations are made, as well as temperature and pressure measurements over time. Eleven K-type thermocouples are located in grooves at the back of the evaporator casing. The operating temperature T_{sat} of the vapor chamber is determined from the mean temperature of two mineral insulated thermocouples, 1.5 mm in diameter, placed inside the chamber. Besides, a Kistler pressure sensor located next to the filling valve measures the operating pressure.

The vapor chamber is alternatively filled with HFE-7100, n-pentane and water. The working fluid is previously degassed in a dedicated container. To minimize the untimely infiltration of non-condensable gas, the evaporator is totally filled, operated at 75-80 W and purged until the required fill charge is reached. A ruler was designed to evaluate the charge very roughly through the transparent cover when the vapor chamber operates, using an arbitrary unit ranging from 0 (empty evaporator) to about 25 (maximum fluid charge), as shown in figure 2. Experiments are carried out varying the heat transfer rate and the fluid charge (uncertainty ± 2). The maximum heat load is not related to thermo-hydraulic phenomena but to the mechanical resistance of the tubes, which limits the pressure and temperature they can sustain.

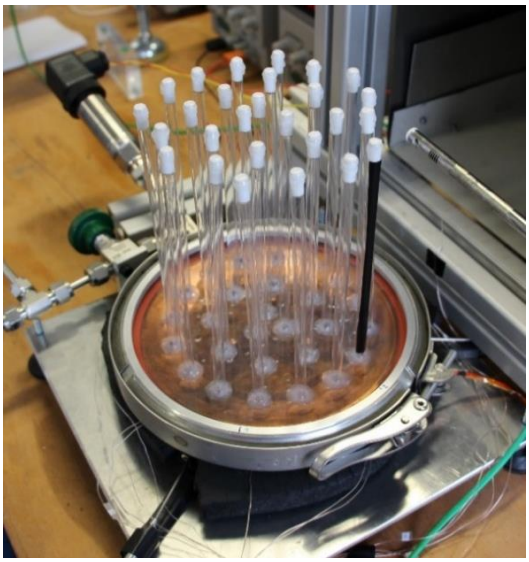

Figure 1. Prototype of thermosyphon vapor chamber with transparent hollow fins.

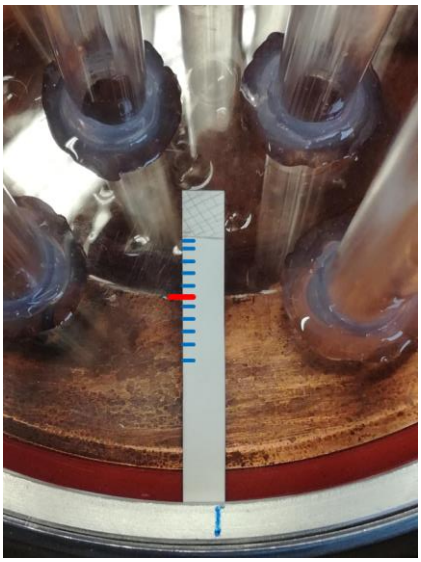

Figure 2. Scaled ruler for fluid charge measurement through the condenser base plate.

2.2. Heat transfer data reduction

A simplified thermal model of the device using an equivalent electrical network is presented in figure 3. It provides the means to evaluate the thermal performances, to compare them for various fluids and fin diameters and to highlight the limiting phenomenon for heat transfer in each case. The global thermal resistance of the vapor chamber is defined using the mean temperature difference between the evaporator and the cooling air at steady state and the total heat transfer rate $\dot{Q}_{tot}$:

$$R_{tot} = \frac{T_{evap,max} - T_{air}}{\dot{Q}_{tot}} \tag{1}$$

where $T_{evap,max}$ is the maximum temperature measured at the evaporator.

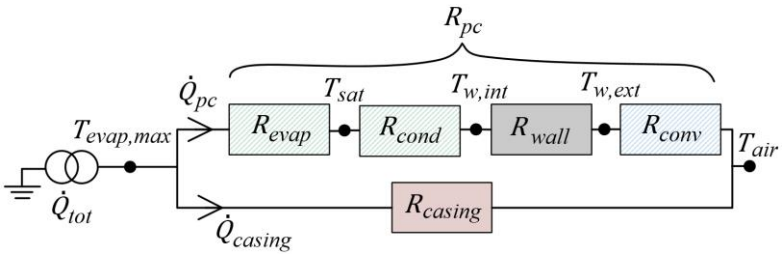

Figure 3. Equivalent electrical network for heat transfer in the vapor chamber.

Despite insulation, part of the heat input is transferred by conduction through the casing, and then convection and radiation. For the present work, it is necessary to estimate the heat flux associated with conduction in the casing $\dot{Q}_{casing}$ in order to properly characterize the impact of the heat effectively transferred by phase change through the condenser $\dot{Q}_{pc}$ on operating regimes. The heat flux $\dot{Q}_{casing}$ depends on the casing resistance, which is evaluated experimentally as the global resistance for the empty vapor chamber:

$$\dot{Q}_{casing} = \frac{T_{evap,max} - T_{air}}{R_{casing}} \quad \text{with} \quad R_{casing} = [0.757(u_{air})^{0.325}]^{-1} \tag{2}$$

The correlation given for R_{casing} is based on regression of experimental data for $1 < u_{air} \leq 3.6$ m/s. Since the air velocity is close to 3.5 m/s for all the considered experiments, R_{casing} is around 0.9 K/W. This value includes convective and radiative heat transfer, as well as conduction through the casing.

The thermal resistance R_{pc} shown in figure 3 (subscript pc stands for phase change) is divided into four resistances according to the heat transfer phenomena involved:

$$R_{pc} = R_{evap} + R_{cond} + R_{wall} + R_{conv} \tag{3}$$

R_{evap} and R_{cond} are associated with phase change in the evaporation and condensation areas. Since the evaporator is 3 mm thick above the heat source and copper thermal conductivity is high, the conduction heat transfer through copper is neglected. R_{wall} is the radial conductive resistance of the polymer wall and R_{conv} is related to forced air convection cooling outside the condenser tubes.

Since the internal wall temperature is unknown, R_{wall} is calculated according to the condenser tube properties and geometry as follows:

$$R_{wall} = \frac{1}{N}\frac{\ln(d_{out}/d_{in})}{2\pi\lambda_{wall}H} \tag{4}$$

where λ_{wall} is the thermal conductivity of the tube wall, N is the number of tubes, H their effective height, d_{in} and d_{out} their inner and outer diameter. The thermal conductivity of the polymer is taken equal to 0.20 W/m.K.

The other resistances are evaluated from the heat load $\dot{Q}_{pc}$ transferred by phase change, the measured temperatures $T_{evap,max}$, T_{sat}, $T_{w,ext}$ and T_{air}, and the radial conductive resistance of the wall

(equation (4)). The mean external wall temperature $T_{w,ext}$ is measured using an infrared camera on a condenser tube covered with an adhesive tape of known emissivity.

3. Results

3.1. Hydrodynamic phenomena and operating regimes

Hydrodynamic phenomena and operating regimes depend on the properties of the tested fluid, especially its capillary length and wettability on the polymer surface. The capillary length of saturated water at 25 °C is 2.7 mm. It is lower for HFE-7100 and n-pentane: their capillary lengths at 25 °C are 0.96 and 1.6 mm, respectively. Therefore, capillary forces compared to gravity ones are the more significant for water then for pentane and next for HFE. These forces can lead to the formation of liquid plugs and also affect their stability.

For HFE-7100 and n-pentane, which perfectly wet the polymer surface, filmwise condensation occurs in the tubes (figure 4a) and there is no liquid plug formation for inner diameters larger than or equal to 5.3 mm. Besides, there is no interaction between evaporator and condenser because, when nucleate boiling appears at the evaporator, the bubbles are too small to reach the condenser. They are indeed a few millimeters in diameter, while the vapor space is 13 mm high. A stable oscillatory regime is observed for all operating conditions. This regime is characterized by stable amplitude and frequency oscillations on the temperature and pressure curves, as shown for pentane in figure 5a. Oscillations are caused by nucleate boiling and condensate drops falling from the condenser to the evaporator. The slow variations also observed on the curves are likely due to fluctuations in the cooling air temperature.

For water as the working fluid, dropwise condensation occurs in the tubes. Water is indeed partially wetting, with a static contact angle of about 60-70°. Besides, the operating pressure with water is between 40 and 160 mbar, which is quite low compared to that measured with HFE and pentane (around 0.5 and 1 bar, respectively). As a result, water vapor bubbles formed at the evaporator are large [7] and often reach the condenser base plate. Due to the interaction between boiling and condensation within the confined space, and depending on the fluid fill charge, the tube diameter and the operating conditions, many intermittent hydrodynamic phenomena can be observed. For all tested diameters, liquid plugs such as the one shown in figure 4b are formed from the base of the tubes and pushed upwards by the vapor flow. For the larger diameters (7.6 and 10.7 mm), plug formation requires liquid supplied from the evaporator. It is provided as a consequence of low pressure boiling: large bubbles force liquid into the condenser tubes. This geyser effect [8] is observed periodically and is higher and more frequent when boiling is intense. Moreover, liquid plug stability increases when the fin diameter is reduced: thin unstable liquid plugs are formed in 10.7 mm tubes, while plugs up to 6-7 cm high can be observed inside 7.6 mm tubes. These large liquid plugs intermittently fall to the evaporator under the effect of gravity forces. For the smallest diameter (d_{in} = 5.3 mm), the stability is sufficient for the liquid to occupy the whole height of the tubes and prevent efficient heat transfer at the condenser. Small fins filled with water are shown in figure 4c. Accumulation of stable liquid plugs inside the fins eventually leads to an evaporator dry out if the fill charge is too low. Lastly, spontaneous flooding of tubes sometimes occurs at high fill charge, for small as well as large diameters.

Figure 4. Illustrations of condensation regimes (a) pentane filmwise condensation, (b) water liquid plug and dropwise condensation inside a 7.6 mm diameter fin, (c) 5.3 mm diameter fins filled with stable water plugs.

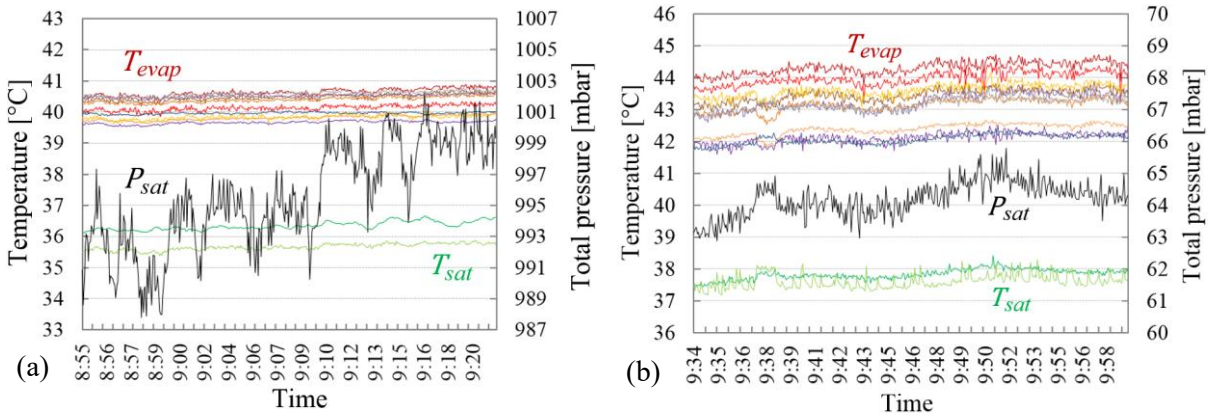

Figure 5. Examples of temperature and pressure signatures of a stable oscillatory regime
(a) pentane, charge 5, d_{in} = 5.3 mm, $\dot{Q}_{pc}/\dot{Q}_{tot}$ = 55 / 75 W,
(b) water, charge 10, d_{in} = 10.7 mm, $\dot{Q}_{pc}/\dot{Q}_{tot}$ = 52 / 80 W.

Figure 6 summarizes the various hydrodynamic phenomena observed in the vapor chamber and their connection with the identified operating regimes (in green color). For HFE and pentane, a stable oscillatory regime is observed whatever the tube size. For water with 5.3 mm diameter tubes, fins are filled with liquid and a stable oscillatory regime is also observed for all tested operating conditions. According to both observations and measurements, two intermittent regimes are defined in addition to the stable oscillatory regime described previously, which is illustrated for water in figure 5b:

- An intermittent "boiling" regime (figure 7) characterized by cyclic increase and decrease in temperatures and pressure, over cycles as short as one to two minutes. Moreover, these parameters are correlated. This regime is likely due to low pressure boiling with intermittent and abrupt formation of large bubbles. Its apparition depends on the heat load and fluid charge. The amplitude of the oscillations is larger in figure 7 (a) than (b) because of a more developed boiling at higher heat flux.
- An intermittent "liquid motions" regime that occurs only when liquid plugs are unstable. It is characterized by the succession of "calm" and "agitated" phases on timescales from a few minutes to several tens of minutes. This behavior is due to liquid motions that increase periodically the effective fluid charge at the evaporator and the impact of confinement on

boiling, such as falls of liquid plugs / columns or a geyser effect (liquid rising from the evaporator) stopping. Examples of temperature and pressure signatures of this regime are presented in figure 8: they are slightly different for 10.7 and 7.6 mm diameter tubes. In the former case, the difference between "calm" and "agitated" phases is observed on the curves thanks to periodic amplitude variations of oscillations whereas, in the latter case, the "agitated" phase is visible during experiments with an increase in the frequency and intensity of thermo-hydraulic phenomena compared to the "calm" phase, but the amplitude of oscillations on the curves remains the same in both phases.

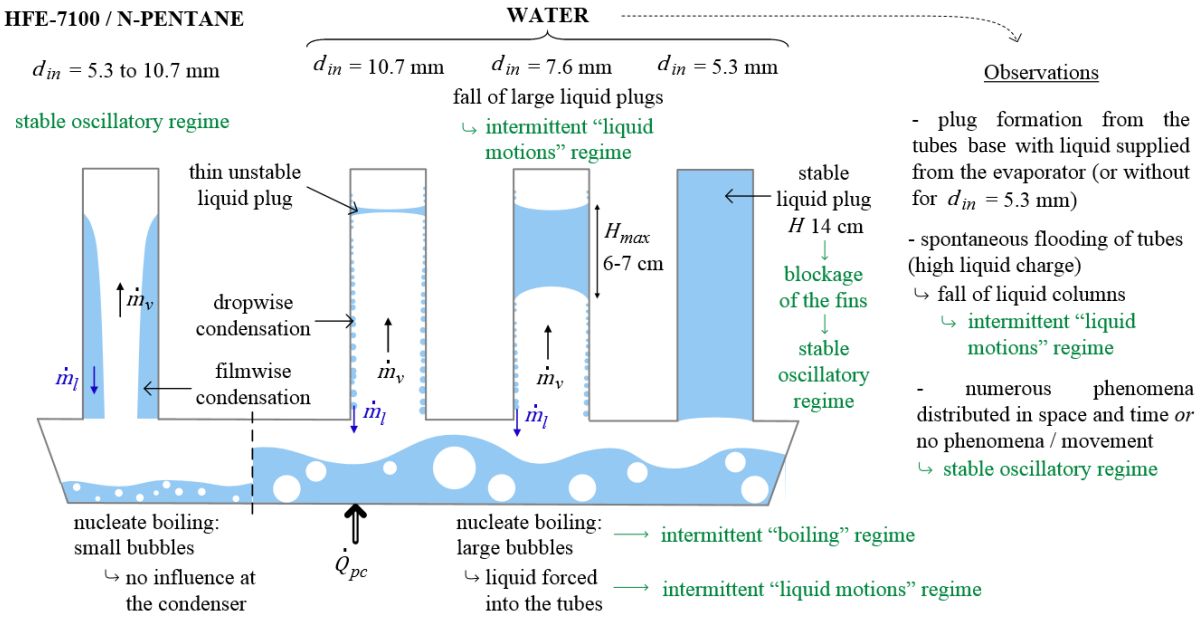

Figure 6. Summary diagram of observed hydrodynamic phenomena depending on the working fluid and fin diameter (not to scale).

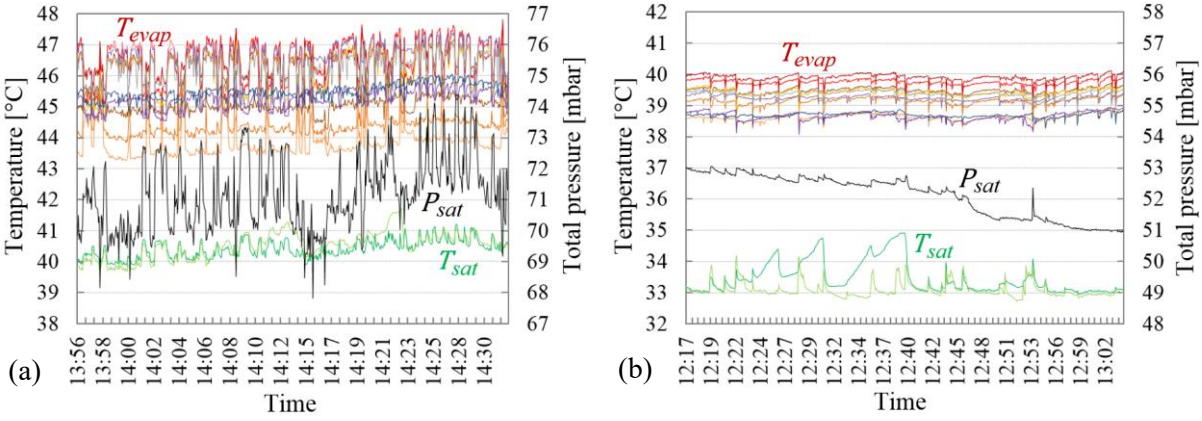

Figure 7. Examples of temperature and pressure signatures of an intermittent "boiling" regime
(a) water, charge 5, d_{in} = 10.7 mm, $\dot{Q}_{pc}/\dot{Q}_{tot}$ = 51 / 80 W,
(b) water, charge 6, d_{in} = 10.7 mm, $\dot{Q}_{pc}/\dot{Q}_{tot}$ = 20 / 40 W.

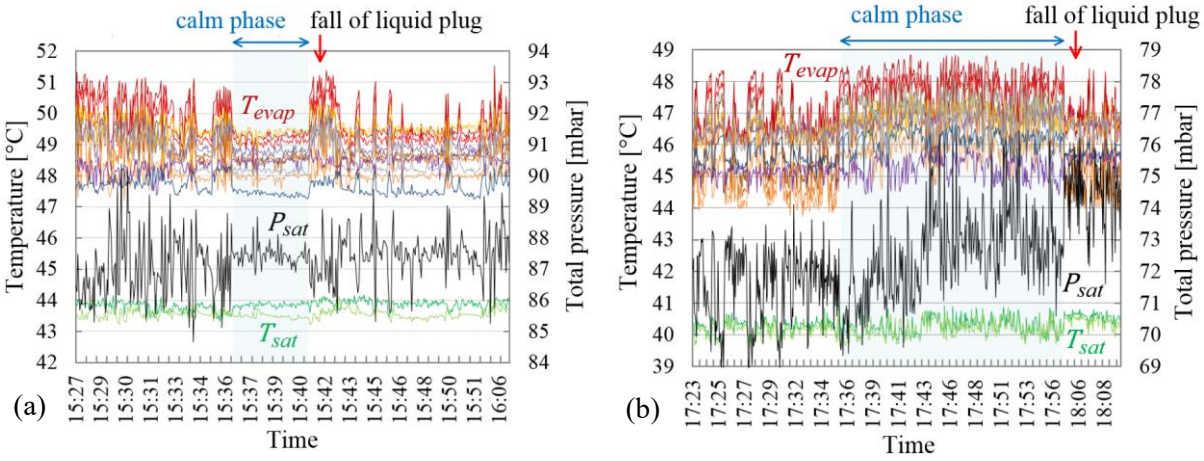

Figure 8. Examples of temperature and pressure signatures of an intermittent "liquid motions" regime (a) water, charge 6, d_{in} = 10.7 mm, $\dot{Q}_{pc}/\dot{Q}_{tot}$ = 64 / 95 W, (b) water, charge 6, d_{in} = 7.6 mm, $\dot{Q}_{pc}/\dot{Q}_{tot}$ = 51 / 80 W.

Regime maps were developed for water in 10.7 and 7.6 mm tubes, as shown in figure 9. The occurrence of a regime depends on the range of fluid charge (horizontal axis) and on the heat transfer rate (vertical axis). The intermittent regimes are sometimes difficult to identify because they can coexist, and their prediction is then even more challenging. As explained before, the intermittent "liquid motions" regime originates from falls of liquid plugs or geyser effect but, when these phenomena are frequent, quite numerous and distributed in time and space, a stable oscillatory regime is observed. The stable oscillatory regime also occurs when the fill charge or the heat load are really low because, in the first case, the boiling liquid does not interact with the condenser (no geyser effect or plug formation) and, in the second case, there is no boiling anymore. Intermittent "boiling" and "liquid motions" regimes appear only above a critical heat load, which is about 20 W for the former and close to 40 W for the latter, when the fluid charge is around 6. The comparison of figure 9 (a) and (b) shows that the stable oscillatory regime occurs over a larger range of fluid charges for the highest diameter whereas, when d_{in} = 7.6 mm, the intermittent "liquid motions" regime prevails. This can be explained by the formation and fall of large liquid plugs, which is much more frequent in the smaller tubes. Moreover, for the larger diameter tubes, a stable oscillatory regime has systematically been observed for fluid charges between 8 and 12. Additional tests are needed to confirm this result and complete the operating regime maps.

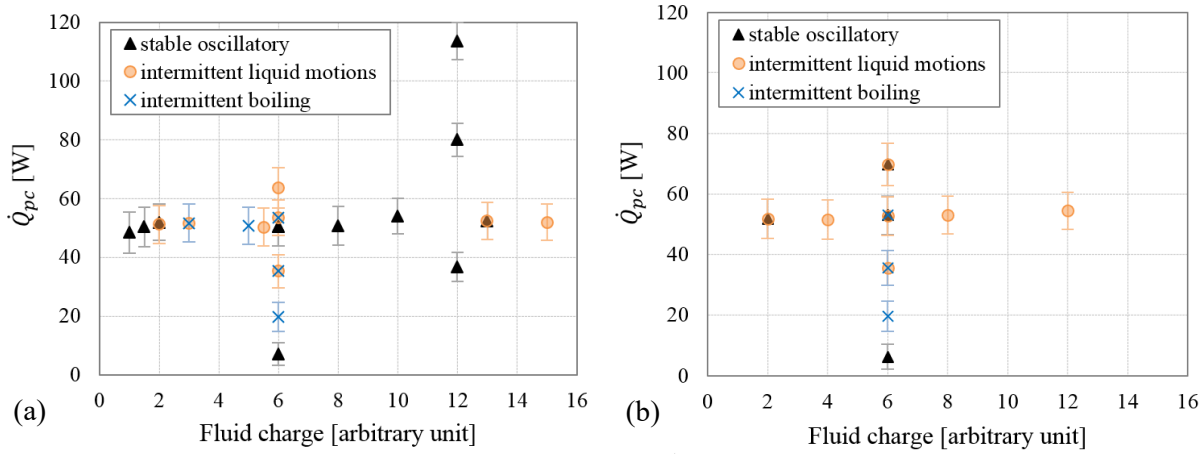

Figure 9. Operating regime maps for water as the working fluid (a) d_{in} = 10.7 mm, (b) d_{in} = 7.6 mm.

3.2. Thermal performance

Figure 10 presents the results obtained for HFE-7100 with 5.3 mm diameter tubes. The evolution of R_{evap}, R_{cond}, R_{wall} and R_{conv}, whose sum is equal to R_{pc}, is shown in figure 10a with respect to the heat load. The evaporation and condensation resistances decrease when $\dot{Q}_{pc}$ increases, while the wall and convective resistances are hardly affected. As a result, the global resistance R_{tot} is reduced when the heat load rises. The casing resistance is also included in figure 10a (red dashed line): it is two to three times higher than R_{tot}. The relative contributions of R_{evap}, R_{cond}, R_{wall} and R_{conv} to R_{pc} are somewhat visible in figure 10a. They are also detailed for the highest tested heat load in the pie chart of figure 10b. The convective cooling resistance is preponderant (47%), followed by R_{evap} (31%). The contribution of R_{wall} is smaller than 10% despite the low thermal conductivity of polymer. The results are comparable when the fin diameter is 10.7 mm. Besides, for experiments with n-pentane, boiling is somewhat more efficient than with HFE, but the evolution of thermal resistances with the heat transfer rate is rather similar, as well as the relative importance of R_{evap}, R_{cond}, R_{wall} and R_{conv}.

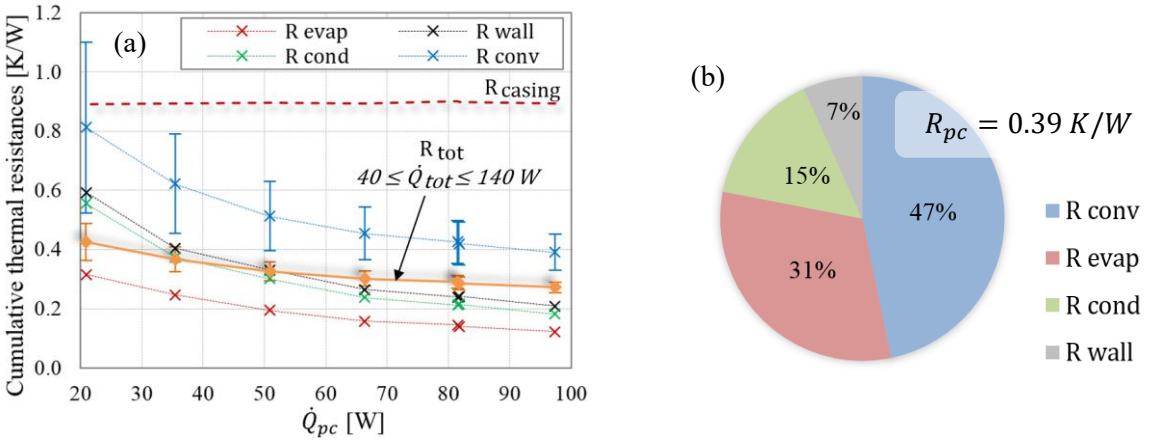

Figure 10. Thermal performance of the vapor chamber filled with HFE-7100 (constant fluid fill charge optimized for the highest tested heat load) for d_{in} = 5.3 mm (a) evolution of the cumulative thermal resistances with the heat load $\dot{Q}_{pc}$ and comparison of R_{tot} and R_{casing}, (b) comparison of relative contributions for the highest tested heat load ($\dot{Q}_{pc}/\dot{Q}_{tot}$ = 97 / 140 W).

For water as the working fluid and 10.7 or 7.6 mm diameter, operating regimes do not seem to influence the performance of the vapor chamber independently of the heat load and fill charge. Air convection cooling is indeed the limiting phenomenon whatever the regime, as shown in figure 11. Besides, reducing the fin diameter from 10.7 to 7.6 mm does not impact the results significantly: the relative importance of the heat transfer phenomena in the thermal resistance is similar in both cases. However, further reduction in the fin size leads to substantial increase in R_{cond} and in the phase change resistance R_{pc} (figure 11c). The influence of the regimes on the thermal performance is thus negligible as long as the fin inner diameter is large enough to prevent the occurrence of stable liquid plugs occupying the whole height of the tubes.

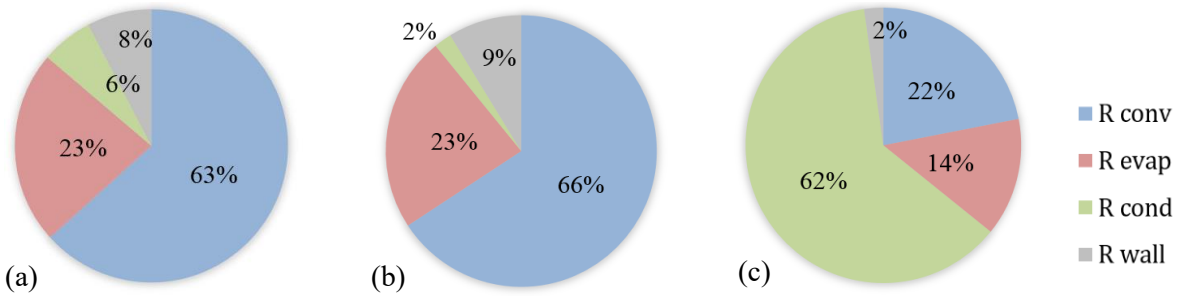

$R_{pc} = 0.41\ K/W$ $R_{pc} = 0.38\ K/W$ $R_{pc} = 1.05\ K/W$

Figure 11. Thermal performance of the vapor chamber filled with water. Comparison of relative contributions for various diameters at the highest tested heat load (a) d_{in} = 10.7 mm, $\dot{Q}_{pc}$ = 64 W, (b) d_{in} = 7.6 mm, $\dot{Q}_{pc}$ = 70 W, (c) d_{in} = 5.3 mm, $\dot{Q}_{pc}$ = 36 W.

The comparison of measured global thermal resistances for the tested fluids and diameters is presented in figure 12 as a function of the total heat load. For all tested conditions, the resistance is reduced when the heat load increases: this reduction is faster for the lowest heat loads and progressively slows down. The fluid fill charge is nearly identical in all cases, except for water in 5.3 mm diameter tubes where it was increased in order to prevent an evaporator dry out. Since the fins are filled with liquid in this case, the performance deteriorates: the increase in R_{tot} is around 50% when reducing the inner diameter from 7.6 to 5.3 mm with water. Leaving this case aside, the global performance obtained with HFE and water is rather similar, but the maximum heat load is lower with water for mechanical reasons (§ 2.1). The best performance is measured with pentane, despite a maximum heat load even lower. This can be explained by a latent heat three times greater than that of HFE, leading to smaller vapor and condensate mass flow rates, and by a low confinement compared to water.

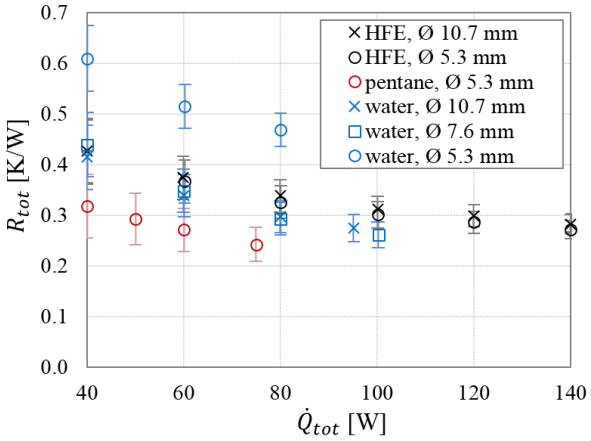

Figure 12. Comparison of the global thermal resistance R_{tot} for the tested fluids and fin diameters.

4. Conclusions

Depending on the working fluid, fill charge and fin diameter, various hydrodynamic phenomena can take place at the condenser of a vapor chamber with hollow fins. Experiments carried out with HFE-7100 and n-pentane showed that filmwise condensation and a stable oscillating regime are observed for all operating conditions. For water, on the other hand, dropwise condensation occurs as well as geyser effect, formation and motion of liquid plugs and flooding of tubes. These phenomena generate intermittent operating regimes and, when reducing the diameter, result in a blocking of condensation in

thin fins that substantially deteriorates the thermal performance. The determination of the minimum diameter is thus greatly important for the optimization of the vapor chamber performance, considering condensation heat transfer as well as external convection. Besides, ways of destabilizing liquid plugs should be explored in order to improve the performance of such systems.

Acknowledgments
This work was supported by the Carnot Institute Ingénierie@Lyon in the frame of the CAPIT4L project.

References

[1] Bulut M, Kandlikar SG and Sozbir N 2019 A review of vapor chambers *Heat Transf. Eng.* **40** 1551–73
[2] Michels V, Milanez FH and Mantelli MH 2007 Analytical model to predict thermal resistances of hollow fin heat sinks *19th Int. Congress of Mechanical Engineering* (Brasilia)
[3] Michels V, Milanez FH and Mantelli MBH 2012 Vapor chamber heat sink with hollow fins *J. Braz. Soc. Mech. Sc. Eng.* **34** 233–7
[4] Tsai T-E, Wu H-H, Chang C-C and Chen S-L 2010 Two-phase closed thermosiphon vapor-chamber system for electronic cooling *Int. Comm. Heat Mass Transf.* **37** 484–9
[5] Ji X, Xu J, Abanda AM and Xue Q 2012 A vapor chamber using extended condenser concept for ultra-high heat flux and large heater area *Int. J. Heat Mass Transf.* **55** 4908–13
[6] Ong KS, Haw PL, Lai KC and Tan KH 2017 Vapor chamber with hollow condenser tube heat sink *AIP Conf. Proc.* **1828** 020018
[7] Giraud F, Rullière R, Toublanc C, Clausse M and Bonjour J 2015 Experimental evidence of a new regime for boiling of water at subatmospheric pressure *Exp. Therm. Fluid Sci.* **60** 45–53
[8] Smith K, Kempers R and Robinson AJ 2018 Confinement and vapour production rate influences in closed two-phase reflux thermosyphons Part A: flow regimes *Int. J. Heat Mass Transf.* **119** 907–921